2011

Automatic Detection of Aircraft Emergency Landing Sites

Yu-Fei Shen
Old Dominion University

Zia-ur Rahman
NASA Langley Research Center

Dean Krusienski
Old Dominion University, dkrusien@odu.edu

Jiang Li
Old Dominion University, jli@odu.edu

Zia-ur Rahman (Ed.)

See next page for additional authors

Original Publication Citation

Shen, Y. F., Rahman, Z. U., Krusienski, D., & Li, J. (2011). Automatic detection of aircraft emergency landing sites. In Z. -U. Rahman, S. E. Reichenbach, & M. A. Neifeld (Eds.), *Visual Information Processing XX, Proceedings of SPIE 8056* (80560H). SPIE of Bellingham, WA. https://doi.org/10.1117/12.882506

Automatic Detection of Aircraft Emergency Landing Sites

Yu-Fei Shen[a], Zia-ur Rahman[b], Dean Krusienski[a] and Jiang Li[a]

[a]Department of Electrical and Computer Engineering, Old Dominion University, Norfolk, Virginia 23529, USA;
[b]Electromagnetics & Sensors Branch, NASA Langley Research Center, Hampton, Virginia 23681, USA

ABSTRACT

An automatic landing site detection algorithm is proposed for aircraft emergency landing. Emergency landing is an unplanned event in response to emergency situations. If, as is unfortunately usually the case, there is no airstrip or airfield that can be reached by the un-powered aircraft, a crash landing or ditching has to be carried out. Identifying a safe landing site is critical to the survival of passengers and crew. Conventionally, the pilot chooses the landing site visually by looking at the terrain through the cockpit. The success of this vital decision greatly depends on the external environmental factors that can impair human vision, and on the pilot's flight experience that can vary significantly among pilots. Therefore, we propose a robust, reliable and efficient algorithm that is expected to alleviate the negative impact of these factors. We present only the detection mechanism of the proposed algorithm and assume that the image enhancement for increased visibility, and image stitching for a larger field-of-view have already been performed on the images acquired by aircraft-mounted cameras. Specifically, we describe an elastic bound detection method which is designed to position the horizon. The terrain image is divided into non-overlapping blocks which are then clustered according to a "roughness" measure. Adjacent smooth blocks are merged to form potential landing sites whose dimensions are measured with principal component analysis and geometric transformations. If the dimensions of the candidate region exceed the minimum requirement for safe landing, the potential landing site is considered a safe candidate and highlighted on the human machine interface. At the end, the pilot makes the final decision by confirming one of the candidates, also considering other factors such as wind speed and wind direction, etc. Preliminary results show the feasibility of the proposed algorithm.

Keywords: Emergency landing, forced landing, hazard detection, horizon detection

1. INTRODUCTION

Engine failure, running out of fuel, extremely bad weather, medical emergency, aircraft hijack are the top five leading factors of unplanned landing, which is also called emergency landing. Particularly, under the two most emergent situations, engine failure and running out of fuel, the aircraft may quickly lose flying power and its maneuverability is restricted to gliding. Once these happen, a forced landing process has to be immediately carried out. If, as is unfortunately usually the case, there is no airport or even a runway that can be reached by the un-powered aircraft, a crash landing or ditching will be inevitable.

Finding a suitable emergency landing site is vital to the survival of passengers and the pilot. Conventionally, the landing site is visually selected by the pilot looking at the terrain that is visible through the cockpit. This is a required fundamental skill in the flight training program, and every pilot is supposed to have the capability to do so. However, many external environmental factors, i.e., fog, cloud, rain, illumination, etc. can significantly affect human vision so that the decision of choosing the optimal landing site highly depends on the pilot's flight experience—the most significant internal factor—which can vary a lot among different pilots. In addition, the visual angle that the human eyes can cover simultaneously is limited: when the pilot looks to the left, what is on the right is missed, and vice versa. Since time is of supreme importance in the scenario we are considering, the inability to scan on both sides of the cockpit simultaneously is a distinct disadvantage. Imaging sensors can

Contact author information:
Yu-Fei Shen: E-mail: yshen002@odu.edu

Visual Information Processing XX, edited by Zia-ur Rahman, Stephen E. Reichenbach, Mark A. Neifeld,
Proc. of SPIE Vol. 8056, 80560H · © 2011 SPIE · CCC code: 0277-786X/11/$18 · doi: 10.1117/12.882506

alleviate this problem by creating panorama images that encompass the entire field-of-view (FOV) in front of the aircraft. Therefore, in order to compensate for the natural inadequacies of human vision and also to alleviate the negative effects of both external and internal factors, a robust, reliable and efficient process for emergency landing site selection is greatly desirable. We proposed an automatic computer-aided detection (CAD) system.[1] In that paper, we firstly investigated the appropriate criteria to assess landing sites. A candidate landing site is considered safe only if its surface is smooth and its length and width are adequate. Then we introduced the system framework and described the modules of measuring the smoothness and the dimensionality of the potential landing sites in details.

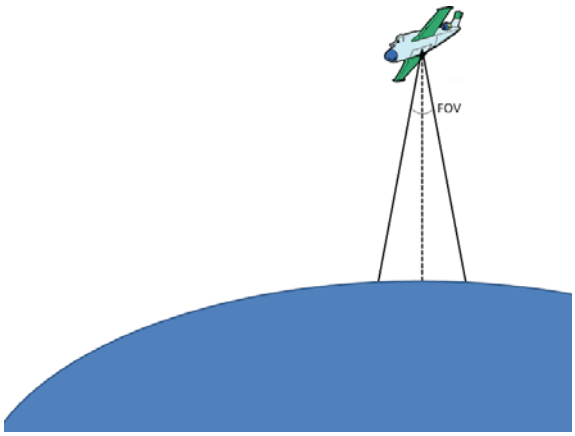

Figure 1: Camera vertically faces down

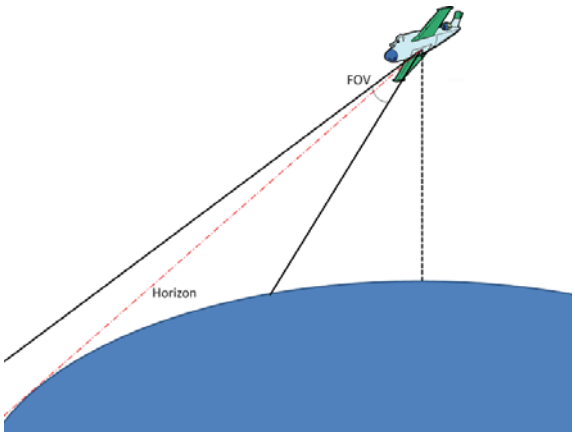

Figure 2: Camera faces forwards

A simplified imaging model was utilized as shown in Figure 1 at the early stage of this research, in which images were vertically acquired. In this paper, we try to utilize images that are captured in a more practical way as shown in Figure 2, since for the gliding un-powered aircraft, a frontal landing site is obviously a better and easier option than a underneath or backward landing site. Due to the change of the view direction, a large area of sky comes into the scene. To avoid the sky being wrongly detected as large and smooth landing site, as an important component of this paper, we present an algorithm of accurate horizon detection that is used to differentiate the earth and the sky. In addition, corresponding to the change of the angle of view, we present the modified mathematic model of the existing CAD system.

Related research has been conducted by many groups in recent years. NASA Jet Propulsion Laboratory (JPL) proposed a LIDAR-based hazard avoidance approach for safe landing on Mars.[2] They made use of elevation maps generated by scanning synthetic terrains with a simulated LIDAR model. Later, JPL introduced a fuzzy rule-based safety index to assess landing sites.[3,4] Furthermore, they brought multi-sensor images into their approach.[5] Based on ballistic analysis, JPL also proposed a method to estimate the reachable area for the spacecraft.[6] In addition to its application to landing on Mars, autonomous landing and hazard avoidance technology (ALHAT) is also utilized for lunar landing[7–9] and unmanned aerial vehicle (UAV) landing.[10] Therefore, the proposed CAD system potentially has a wide range of applications.

The remainder of the paper is organized as follows. We detail the horizon detection algorithm and the modified mathematic model in Section 2. Preliminary testing results are shown in Section 3. The conclusions are drawn in Section 4.

2. METHODS

Surface roughness and dimensionality, as discussed in our previous paper,[1] are two very important attributes of a landing site, which will directly determine the safeness of an emergency landing. In general, the undulation of terrain can reflect its roughness to some extent, so it seems plausible that if the elevation map of the terrain is known, then its gradient information can be obtained and its roughness can be reasonably estimated. However, in the specific scenario of this research, the safeness of emergency landing is not only determined by the elevation variation of the land but also threatened by the hazards upon the ground, i.e., trees, rocks, vehicles, etc., which are

usually not captured in the elevation database. Therefore, a vision-based information channel is indispensable, which provides the real-time imagery of the ground. Ideally, when the aircraft is flying in the upper air, it can be guided to a roughly smooth area according to the gradient information derived from the elevation map. Then, the proposed CAD system leads the aircraft to a safe emergency landing site. In practice, most of aircrafts do not have either the database of elevation maps or the LIDAR sensor system. Imagery captured by aircraft cameras is the only available information source so that the proposed CAD system will play a crucial role under this scenario.

A primary and straightforward imaging model as shown in Figure 3 was utilized in our previous paper[1] to test the feasibility of the proposed CAD system, and preliminary but promising results were achieved. In this paper, we expand the study to a deeper level by introducing a forward-looking imaging model illustrated in Figure 4, which provides more accessible options to the un-powered gliding aircraft. In addition, the computational model involved in measuring the dimensionality of potential landing sites is improved according to the change of the angle of view.

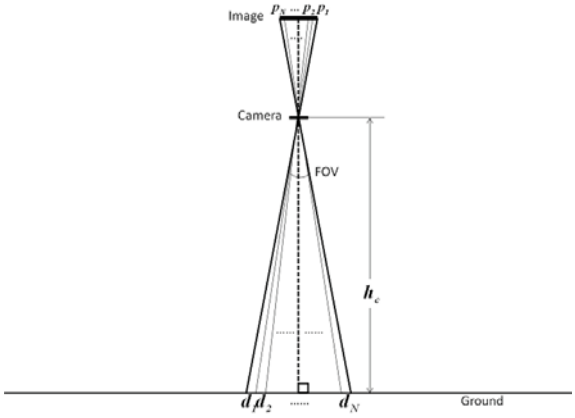

Figure 3: Imaging model in our previous paper

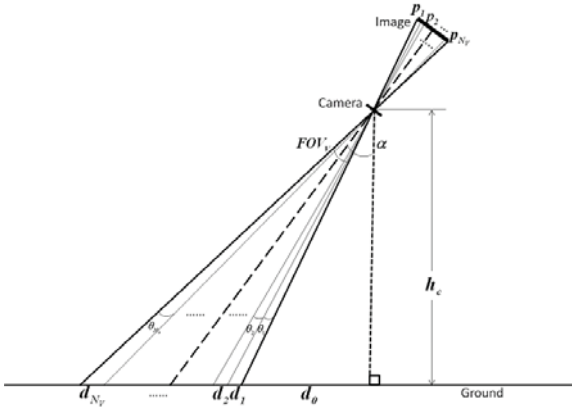

Figure 4: Improved imaging model

In the forward-looking imaging model, the sky comes to the image scene, and it is necessary to differentiate the sky from the earth, otherwise the CAD system may mistake the sky as a smooth and large area. An automatic horizon detection algorithm is proposed to solve this problem, which is detailed as follows. First of all, the original image as shown in Figure 5 is blurred by a large scale Gaussian low-pass filter so that all the fine edges are ignored and only strongest bounds are retained as shown in Figure 7. Secondly, an edge detector is utilized to find the major bounds. In this paper, we make use of the Canny edge detector[11] because it can provide edge strength information in addition to edge location information. Based on the edge strength of each pixel of the image, a edge strength histogram is computed and top $p\%$ of the points are obtained as possible points of the horizon. It is worthy to note that the edge strength threshold is adaptive for different images. The value of p should be a small number, because by experience we know the horizon is the strongest bound in the image most of the time. However, it is not always the case, so the value of p should not be too small. In other words, we would rather conservatively include some un-horizontal points in this step and exclude them in a later step than hastily lose the horizontal points in this step. By experiments, we set

$$p = \frac{1}{N_H} \times 500, \tag{1}$$

where N_H is the total number of pixels along the horizontal direction in the image. Based on the p value and the correspondent edge strength threshold, a binary map can be generated, in which the edges are high-lighted in white color as illustrated in Figure 9. Then, the standard Hough transform (SHT)[12] is applied to search probable lines in the binary map. Ideally the horizon should be the highest peak of the voting result of SHT so that by taking the highest peak value we can find the slope and intercept of the horizon in the image, but it is not always the highest peak. Therefore, we cannot just simply take the highest peak as horizon. Instead, we take into account the top N_L highest peaks by comparing the average edge strength within the dual-side narrow bands

along the N_L lines. The line that has the highest average edge strength within the dual-side narrow bands is called the true peak of Hough transformation. By experiments, we set N_L to 5. This step makes the use of SHT more reliable and robust. In Figure 9, the green line is the true peak of Hough transformation. Since the horizon is not often a strictly straight line, the Hough transformation result may not perfectly match the real horizon. Therefore, it is necessary to adjust the line in a pixel-wise fashion by searching the dual-side neighborhood of each pixel. The coarse adjustment as shown in Figure 9 is applied based on the edge map of the blurred image. The sub-figure inside Figure 9 provides a closer view at a local segment. The yellow arrows denote the directions of adjustment and the red dots denote the position of each horizontal pixel after the coarse adjustment.

After coarsely finding the position of horizon, we get back to the original image and do a fine adjustment to accurately locate the horizon as shown in Figure 10. For each pixel of the coarsely found horizon rendered in green, we search its dual-side narrow band in a fine edge map rendered in a gray scale, which is computed from the original image, and then slightly adjust its position to the pixel that has the largest edge strength of that neighborhood. Yellow arrows point to the directions of adjustment and red points denote the position after the fine adjustment. Noisy points may emerge due to the discontinuity of the horizon in the fine edge map. We remove these discontinuous points by interpolation based on their neighboring points on the left and right. After removing all the noisy points, a smoothing technique is applied to get smooth final detection result as shown in Figure 6. In this paper, we used B-Spline interpolation method.[13,14]

Given the horizon, a mask of ground can be generated and then we apply our automatic emergency landing site detection algorithm[1] to the ground part of the image. The major steps utilized in this paper are consistent with the steps presented in our previous paper.[1] First, we compute the edge strength of each pixel, which ranges from 0 to 255, by using Canny edge detector.[11] Second, we compute the cumulative hazard strength (CHS) of each block, i.e. ten-by-ten pixels. Third, we cluster the blocks to a number of classes based on their CHS as shown in Figure 11. The number of classes is automatically determined by the K-mean clustering method.[15,16] Forth, based on the clustering result, adjacent blocks with the lowest class of CHS are merged to areas as shown in Figure 12. After trimming the narrow branches,[17] potential landing sites are obtained. In the last, the realistic dimensionality of each potential landing site is measured by an improved mathematic model. In flight dynamics, changing the orientation of the aircraft to any direction can be decomposed to three kinds of rotations: yawing, rolling and pitching, which are respectively to rotate the aircraft along the vertical axis, the longitudinal axis, and the lateral axis. Given those three rotation angles, this procedure can be described by the intrinsic or extrinsic matrices composition[18,19] with which one can map the world coordinate system to the aircraft coordinate system, and vice versa. In other words, two arbitrary points in an aerial image can be mapped to the world coordinate system so that the realistic distance between the two points on the ground is measurable if the three rotation angles are known. In practice, many aircrafts have the device to record the three angles so that they can be synchronically restored with real time aerial images. We use images downloaded from Google Earth®in this paper instead of images captured by aircraft-carried cameras. In the lack of the information of the three rotation angles, we simplify the imaging process with only pitching but no yawing and rolling. Therefore, the imaging model in the vertical direction of the image coordinate system can be described as Figure 4, then the realistic size of each pixel along the vertical direction of the image can be calculated as follows,

$$\begin{aligned} d_0 &= h_c \cdot \tan(\alpha - \tfrac{FOV_V}{2}), \\ d_i &= h_c \cdot \tan(\alpha - \tfrac{FOV_V}{2} + \sum_{j=1}^{i} \theta_j) - \sum_{k=0}^{i-1} d_k, \end{aligned} \tag{2}$$

where h_c is the height of camera, α is the pitching angle, FOV_V is the field of view along the vertical direction of the image, N_V is the total number of pixels along the vertical direction, d_0 is the distance between the vertical line and the first pixel, θ_i and $d_i (i = 1, 2, ..., N_V)$ are respectively the angle and the realistic distance corresponding to pixel p_i along the vertical direction. For large N_V, $\theta_i (i = 1, 2, ..., N_V)$ can be considered to have the same

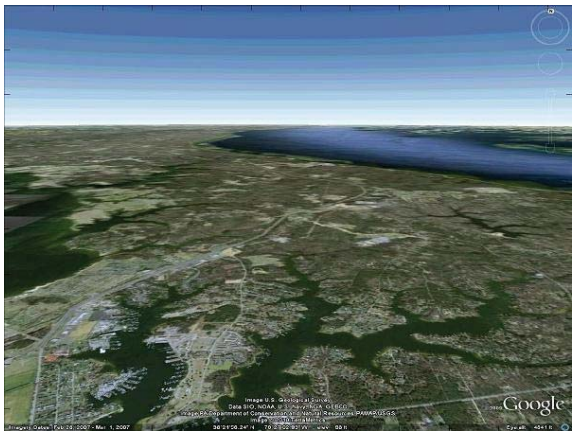

Figure 5: A sample image

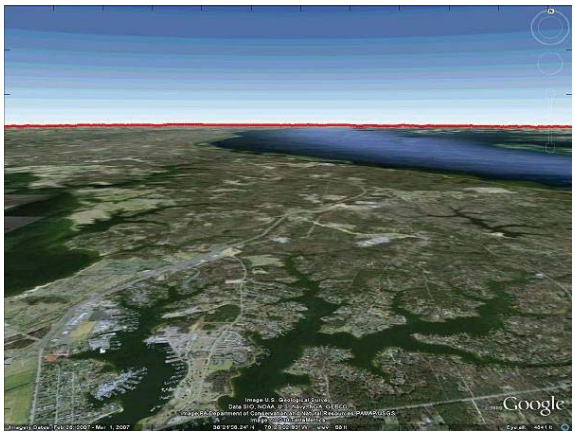

Figure 6: Detected horizon

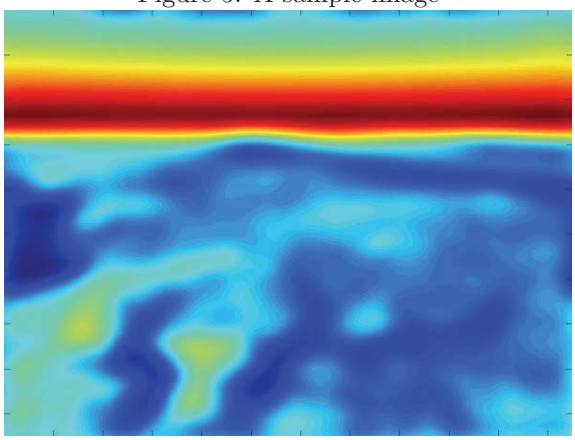

Figure 7: Blurred image

Figure 8: Major edges in the image

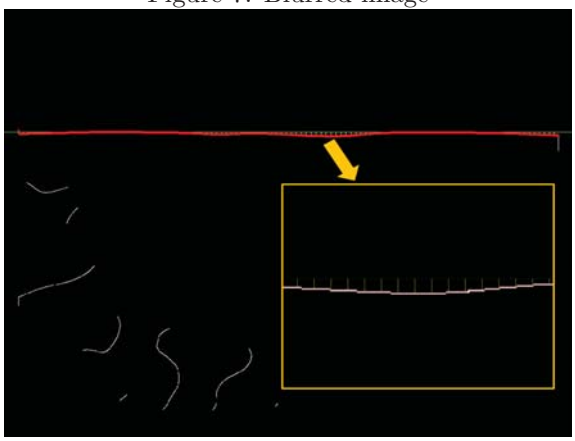

Figure 9: Coarse adjustment

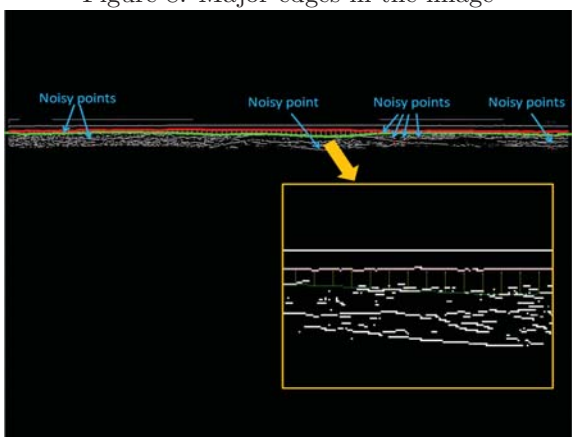

Figure 10: Fine adjustment

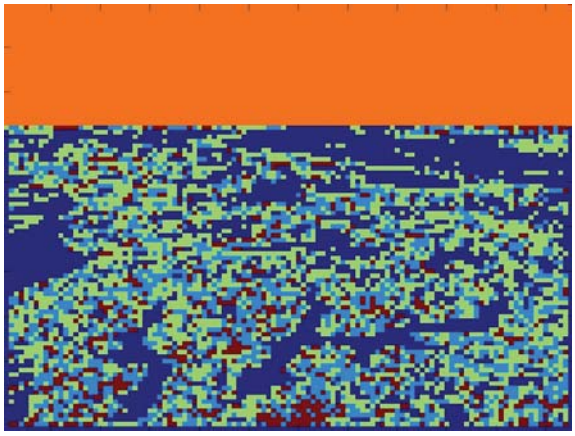

Figure 11: Clustering result based on CHS

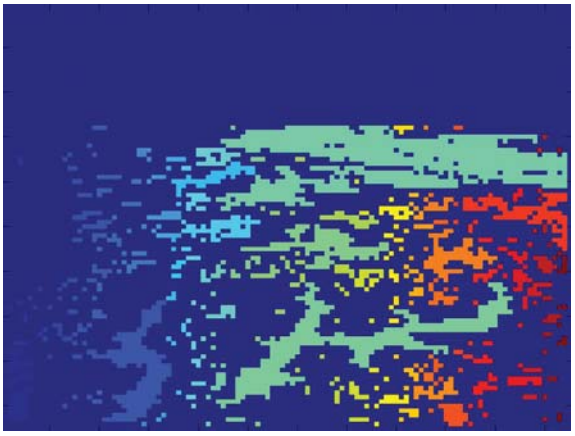

Figure 12: Multi-region growing result

Figure 13: Measurement of realistic dimensionality

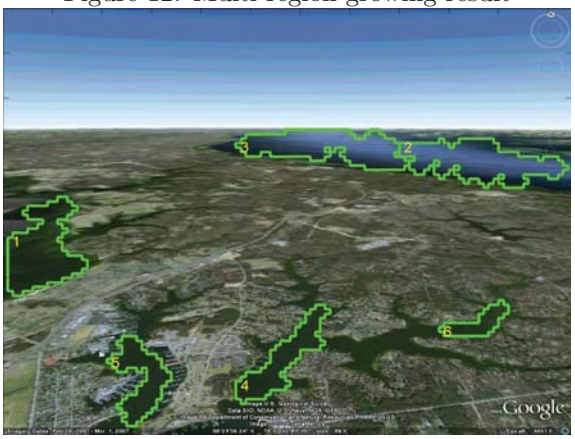

Figure 14: Candidate sites for emergency landing

approximate value θ so that Equation (2) can be simplified as

$$\begin{aligned} d_i &= h_c \cdot \tan(\alpha - \tfrac{FOV_V}{2} + i\theta) - \sum_{k=0}^{i-1} d_k, \\ \theta &= \tfrac{FOV_V}{N_V}. \end{aligned} \tag{3}$$

In addition, since it is assumed that there is no yawing or rolling rotation, the realistic size of pixels along the horizontal direction of the image is the same,

$$d_H = \tfrac{2h_c}{N_H} \tan(\tfrac{FOV_H}{2}), \tag{4}$$

where FOV_H is the field of view along the horizontal direction of the image, N_H is the total number of pixels along the horizontal direction.

The dimensionality of each potential landing site is estimated by measuring the major axis and minor axis of its best fit ellipse, which are obtained by the principle component analysis method. Once the major axis and the minor axis are found, the realistic length L and width W in the unit of feet can be gained as,

$$\begin{aligned} L &= \sqrt{(d_H(x_{a2} - x_{a1}))^2 + (\sum_{k=y_{a1}}^{y_{a2}} d_k)^2}, \\ W &= \sqrt{(d_H(x_{b2} - x_{b1}))^2 + (\sum_{k=y_{b1}}^{y_{b2}} d_k)^2}, \end{aligned} \tag{5}$$

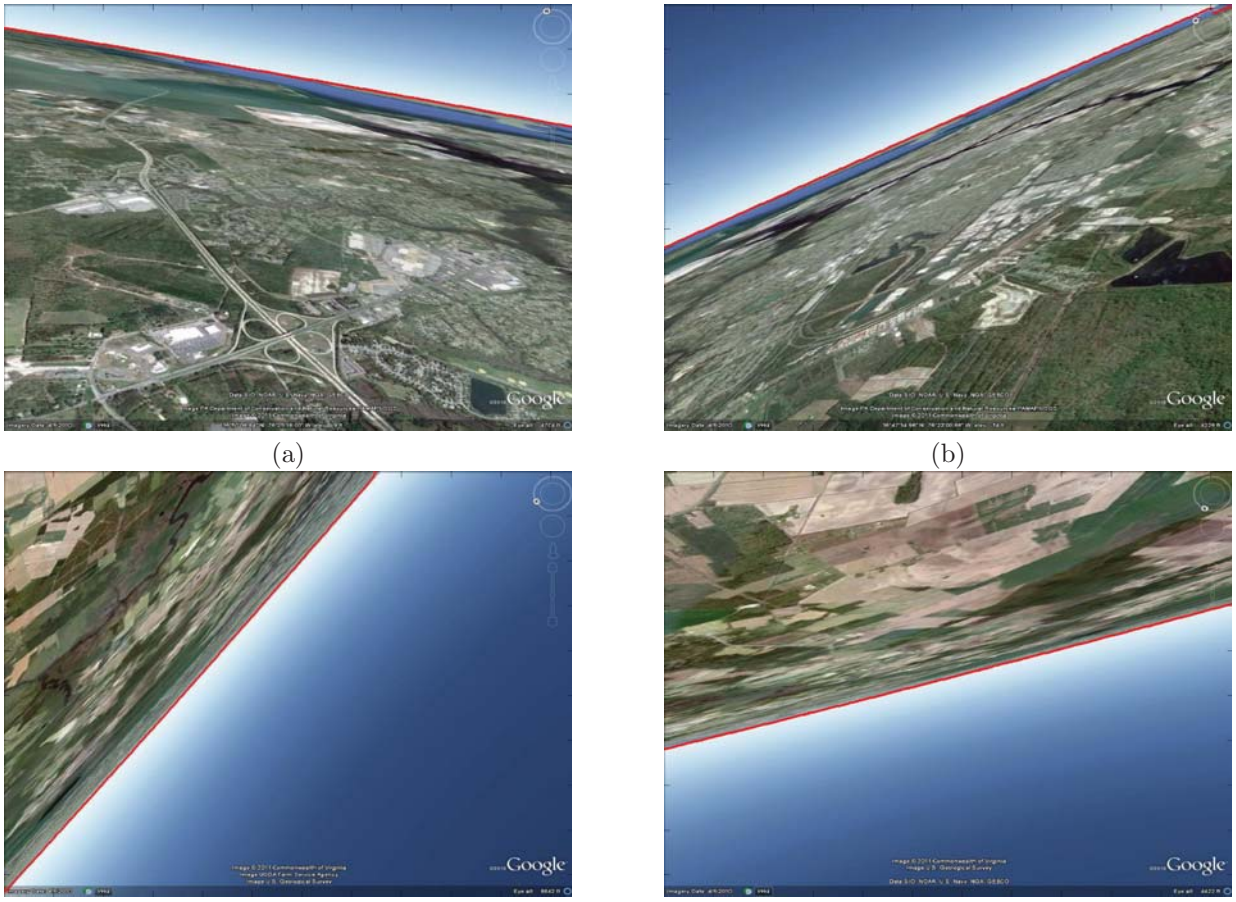

Figure 15: Results produced by the proposed horizon detection algorithm

where (x_{a1}, y_{a1}), (x_{a2}, y_{a2}) are coordinates of two end points of the major axis and (x_{b1}, y_{b1}), (x_{b2}, y_{b2}) are coordinates of two end points of the minor axis, in the image coordinate system. Figure 13 shows the length and width of each potential landing sites. Small areas with insufficient length or width have to be ruled out, and only large areas with sufficient length and width can be considered safe emergency landing sites. In addition, all the candidates landing sites are high-lighted in the human machine interface and labeled with preference indices, which are sorted in a descending order based on their areas, so that the pilot can efficiently evaluate the recommended candidates in the rational order, since the time cost of making a decision is very critical. Finally, the pilot will make his decision by choosing one emergency landing site from recommended candidates, which are high-lighted in green color in the original image, as shown in Figure 14. The priority class of recommendation is reflected by the index number of each candidate landing site, based on the descending order of their areas. In general, larger areas are preferable compared with smaller ones.

3. RESULTS

We tested the proposed automatic horizon detection algorithm on 108 sample images downloaded from Google Earth®and the accuracy reached 100%. The horizon in the 108 sample images appear in various angles and those images are captured at different elevations which ranges from 1000 ft to 20000 ft. We got correct detection results for all of those testing images. Some are shown in Figure 15, in which the red line represents the detected horizon. The robustness and reliability of the proposed automatic horizon detection algorithm is achieved by its hierarchical detection strategies from the coarse detection to the fine adjustment.

To evaluate the detection results of the proposed CAD system, we first asked some skilled pilots to manually

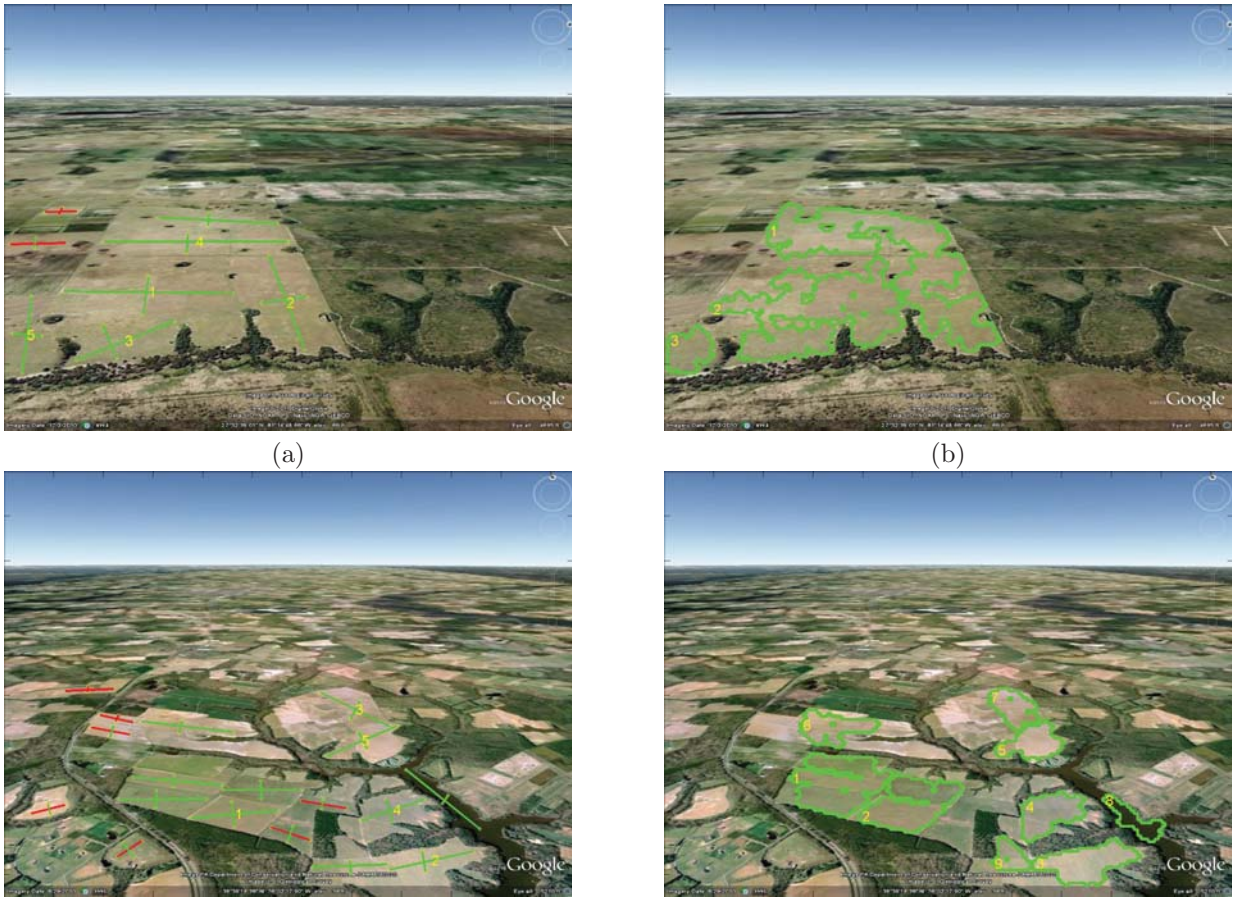

(a) (b)

(c) (d)

Figure 16: (a)(c)Manually selected landing sites; (b)(d)Landing sites recommended by the CAD system

pick all the possible landing sites in the images. Their judgment is mainly based on the apparent smoothness of the areas shown in the images. Next, the dimensions of these manually selected areas are measured by a computer program. This step is necessary because it is hard to accurately estimate the length and width of candidate landing sites in the images captured at different heights by just looking at them. If the dimensions of a selected area meet the minimum requirement, it is rendered in "green" as a safe landing site. Otherwise, it is rendered in "red" as an unsafe landing site. After manual selection, all the selected regions are sorted in a descending order according to area. Only five largest areas are retained as the most suitable landing sites. These manually selected and labeled regions are considered to be the ground-truth with which we compare the results produced by the proposed CAD system. The left column of Figure 16 shows two samples of the labeled manual selection, and the right column shows the corresponding results produced by the CAD system. The emergency landing sites recommended by the CAD system are consistent with the manually selected landing sites. In addition, we also developed a scoring mechanism to quantitatively evaluate the detection results generated by the CAD system, which is utilized to demonstrate the accuracy and reliability of the CAD system.[1] For the future work, we will try to remove the effect of pseudo boundaries inside smooth areas, i.e. an area may be flat but changes in soil color or surficial texture appear as sharp edges that can confuse the CAD system. Therefore, if we are able to recognize the typical textures for different types of terrains, the pseudo edge effect will be possible to be eliminated.

4. CONCLUSIONS

This paper expand the study of our previous paper in which we proposed an automatic CAD system for robust, reliable, and efficient emergency landing site detection. The proposed CAD system makes up for the limitations of human eyes, assists the pilot to find safe landing sites, and more importantly it saves time for the pilot under emergency conditions to devote to other necessary activities. We improved the CAD system in this paper by changing the view angle of the camera and consequently proposed a robust automatic horizon detection algorithm. The horizon detection method achieves a high accuracy performance. In addition, the measurement of realistic dimensionality of the emergency landing site with the improved imaging model is also presented in this paper. The promising results show the feasibility of the proposed CAD system. In the next step, the proposed CAD system will be further developed to better meet practical demands and applications.

Acknowledgments

The authors wish to thank the NASA Aviation Safety Program for the funding which made this work possible. A significant portion of the work was supported under NASA cooperative agreement NNL07AA02A with ODU.

REFERENCES

[1] Shen, Y. and Rahman, Z., "An Automatic Computer-aided Detection System for Aircraft Emergency Landing," in [*Proceedings of the 2011 AIAA Infotech at Aerospace Conference, St. Louis, MO*], 948710 (2011).

[2] Johnson, A., Klumpp, A., Collier, J., and Wolf, A., "Lidar-based hazard avoidance for safe landing on Mars," in [*Proceedings of the 11th Annual AAS/AIAA Space Flight Mechanics Meeting, Santa Barbara, CA*], 323–337 (2001).

[3] Howard, A. and Seraji, H., "A fuzzy rule-based safety index for landing site risk assessment," in [*Automation Congress, 2002 Proceedings of the 5th Biannual World*], 579–584 (2002).

[4] Howard, A., "A novel information fusion methodology for intelligent terrain analysis," in [*Proceedings of the 2002 IEEE International Conference on Fuzzy Systems, 2002 (FUZZ-IEEE'02)*], 1472–1475 (2002).

[5] Howard, A. and Seraji, H., "Multi-sensor terrain classification for safe spacecraft landing," *IEEE Transactions on Aerospace and Electronic Systems* **40**(4), 1122–1131 (2004).

[6] Ploen, S. R., Seraji, H., and Kinney, C. E., "Determination of spacecraft landing footprint for safe planetary landing," *IEEE Transactions on Aerospace and Electronic Systems* **45**(1), 3–16 (2009).

[7] Paschall, S., Cohanim, B. E., Brady, T., and Sostaric, R., "A self contained method for safe & precise lunar landing," in [*IEEE Aerospace Conference, Big Sky, MT*], 1–12 (2008).

[8] Cappellari Jr, J. O., "Where on the moon? An Apollo systems engineering problem.," *Bell System Technical Journal* **51**, 961–1126 (1972).

[9] Solar System Exploration Division, N. J. S. C., "A site selection strategy for a lunar outpost: Science and operational parameters." Conclusions of a Workshop (August 1990).

[10] Fitzgerald, D., Walker, R., and Campbell, D., "A Vision Based Forced Landing Site Selection System for an Autonomous UAV," in [*ISSNIP*], (December 2005).

[11] Canny, J., "A computational approach to edge detection," **8**(6), 679–698 (1986).

[12] Duda, R. O. and Hart, P. E., "Use of the hought transformation to detect lines and curves in pictures," *Communications of the ACM* **15**, 11–15 (January 1972).

[13] Rueckert, D., Sonoda, L. I., Hayes, C., Hill, D. L. G., Leach, M. O., and Hawkes, D. J., "Nonrigid registration using free-form deformations: Application to breast mr images," *IEEE Transactions on Medical Imaging* **18**, 712–721 (Aug 1999).

[14] Lee, S., Wolberg, G., and Shin, S. Y., "Scattered Data Interpolation with Multilevel B-Splines," *IEEE Transactions on Visualization and Computer Graphics* **3**, 228–244 (1997).

[15] Tou, J. T. and Gonzalez, Rafael C., P., [*Pattern Recognition Principles*], Addison-Wesley, Reading, MA (1974).

[16] Duda, R. O. and Hart, P. E., [*Pattern Classification and Scene Analysis*], John Wiley and Sons, New York, NY (1973).

[17] Gonzalez, R. C. and Woods, R. E., [*Digital Image Processing*], Pearson Prentice Hall, Upper Saddle River, New Jersey 07458, third ed. (2008).
[18] Goldstein, H., [*Classical Mechanics*], Addison-Wesley, Reading, MA, 2nd ed. (1980).
[19] Landau, L. and Lifshitz, E. M., [*Mechanics*], Oxford, 3rd ed. (1996).